ELECTROMAGNETIC AND MULTI-PARTICLE BEAM DYNAMICS MODELING OF 4-ROD RFQS

S.S. Kurennoy, R.W. Garnett, L.J. Rybarcyk, LANL, Los Alamos, NM 87545, USA

Abstract

In anticipation of a new RFQ-based front end for the LANSCE linac, we performed a detailed study of the recently commissioned FNAL 4-rod RFQ with the CST Studio. The RFQ model is based on the fabrication CAD files imported into CST. The electromagnetic (EM) analysis was done with MicroWave Studio (MWS) and the beam dynamics modeled with Particle Studio (PS) using the MWS-calculated fields. Realistic matched CW input beam distributions, generated externally with up to 10K particles per RF period and up to 70 RF periods long, were injected into the RFQ for PS simulations. Our simulations reveal some interesting features of 4-rod RFQs. In particular, the end-gap longitudinal field, which is not predicted by standard design codes, can change the output beam energy. Our modeling results helped explain and successfully resolve some problems encountered in the FNAL RFQ commissioning. We plan to use a similar approach to evaluate the new LANSCE 4-rod RFQ.

INTRODUCTION

We are moving forward towards replacing our aging Cockcroft-Walton (C-W) injectors with an RFQ-based front end [1] for the LANSCE proton linac. Based on cost and success of the ISIS C-W-to-RFQ replacement, we have selected a 4-rod type RFQ, although experience at LANL has been mostly with 4-vane RFQs. Therefore, to be better prepared for this upgrade, we studied a 4-rod RFQ recently commissioned at FNAL [2]. Many parameters of the FNAL RFQ are similar to our requirements: 201.25-MHz operating frequency, 35-keV input energy, and 750-keV final energy, – except for the duty factor: 0.12% at FNAL but up to 15% at LANL. The FNAL 4-rod RFQ was designed at IAP (Frankfurt) and manufactured by Kress GmbH, see in [2]. We used the RFQ CAD file imported into CST Studio [3] to create RFQ models and study its performance.

FNAL RFQ MODELS

The imported CAD model was simplified for the EM analysis by removing nonessential details such as external supports, bolts, seals, etc. The RFQ cavity walls were also removed, leaving only the resonator vacuum volume in the CST models. The spring contacts that connect the RFQ stems and tuner plates were replaced by equivalent continuous inserts. The resulting base model is shown in Fig. 1; the 120-cm-long vacuum vessel is shown in light-blue. The inset, a transverse cut through the middle of an RFQ cell between two stems, also indicates the physical orientation of the RFQ vanes as installed at FNAL. The tuners electrically short two adjacent stems and can be moved along them to adjust the mode frequency and voltage profile (flatness) along the structure length.

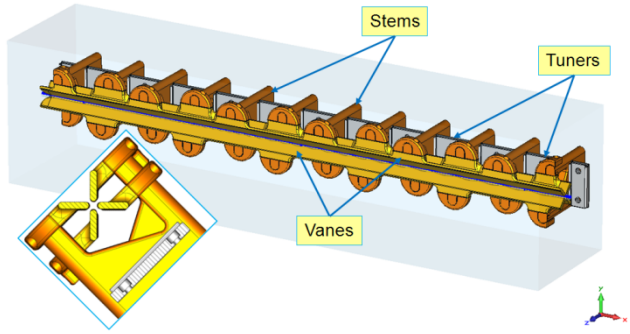

Figure 1: MWS model of the FNAL RFQ.

We studied three different RFQ models with the CST MicroWave Studio (MWS). Model A includes large beam pipes of 10-cm diameter attached to the vacuum box; the tuners are adjusted in MWS simulations. Model B has short and narrow 15-mm-diameter beam pipes; the tuner positions are from FNAL measurements. It corresponds to the RFQ box closed by two end plates with narrow holes. The longitudinal cross sections of the two models are shown in Fig. 2. In B the tuners in five cells are extended by adding half-cylinders ("half-moons") to avoid moving the tuner plates above the stem cuts.

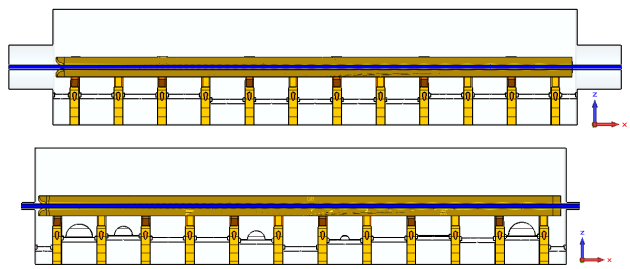

Figure 2: RFQ models A (top) and B (bottom).

Both models A and B have thick vanes that were replaced in July 2012 by thinner vanes to raise the frequency. This final layout, which still has 2 medium and 2 small half-moons, corresponds to our model C; the tuner positions are as tuned at FNAL. This model has the same large beam pipe as model A at its downstream end but a smaller one upstream, with diameter 31.75 mm. More details can be found in reports [4, 5].

EM ANALYSIS

The mode frequencies and RF fields in the RFQ cavity are calculated using the MWS AKS eigensolver that provides more accurate surface approximations. The more efficient tetrahedral solver fails due to the complicated vane shapes. Here we present only some interesting features of the RF fields; see more in [4].

ISBN 978-3-95450-122-9

The first is the presence of a small transverse horizontal (parallel to the ground plane) electrical-field component, E_y, on the RFQ geometrical axis, sometimes referred to as a "dipole" component. This is due to the transverse electric fields being stronger between two upper vanes than between two lower ones, which results in the center of the transverse quadrupole field pattern displaced down from the geometrical axis by 0.5 mm. The shift is small but not negligible when compared to the 3-mm vane aperture. The effect is known in 4-rod RFQs designed for higher frequencies, see [6]. The electric-field components on axis: E_x – longitudinal, E_y, and E_z – vertical, along the stems, – are plotted in Fig. 3 versus the longitudinal coordinate x for model C. The fields are scaled to the nominal inter-vane voltage V_0=72 kV. In a similar plot along the axis shifted by -0.5 mm in z, the component E_y is close to zero, while the two others do not change [4].

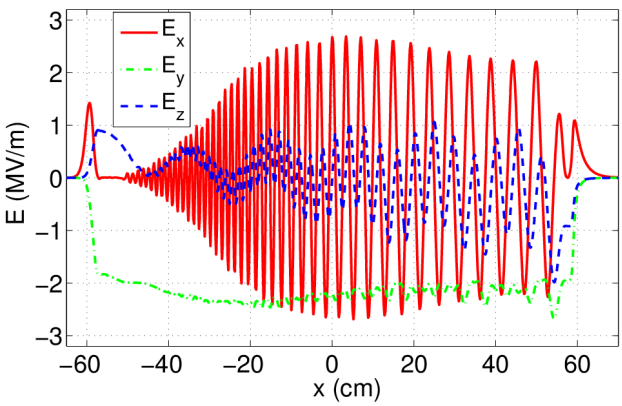

Figure 3: On-axis electric field in RFQ model C.

Another important feature is the longitudinal electric field in the end gaps that separate the vane ends from the RFQ box walls (end-gap bumps). The red curve E_x in Fig. 3 shows the RFQ accelerating field – the oscillating part – that is produced by the vane modulation, but also has two peaks, near the entrance and exit. The RFQ cavity extends from x = -60 cm to x = 60 cm; the vanes start at -59.3 cm and end at 58.87 cm, so that the entrance gap is 7 mm and exit gap is 11.3 mm long. Note that fields extend into the beam pipes. The end-gap longitudinal field exists because the quadrupole symmetry is broken near the RFQ ends; it vanishes in a perfectly symmetric structure like a 4-vane RFQ. 3-D electrostatic computations with vanes charged as a quadrupole do not exhibit bumps since the field is quad-symmetric [4]. One should note that even in 4-vane RFQs with vane cuts that distort the symmetry (e.g., in split-coaxial structures), the end-gap peaks are present [7]. The end-gap bumps depend on the diameter of beam pipes attached to the RFQ as illustrated in Fig. 4, where models A and B are compared. The accelerating fields coincide well in the two models. In case B, the narrow beam pipes trap the fields in the gaps, so the peaks are higher and shorter. In case A without vane modulation (green curve) there is no accelerating field, as expected, but the end-gap bumps are the same as with modulation. Under some circumstances the end-gap fields, which are neither predicted nor taken into account by standard RFQ design codes, can change the exiting beam parameters.

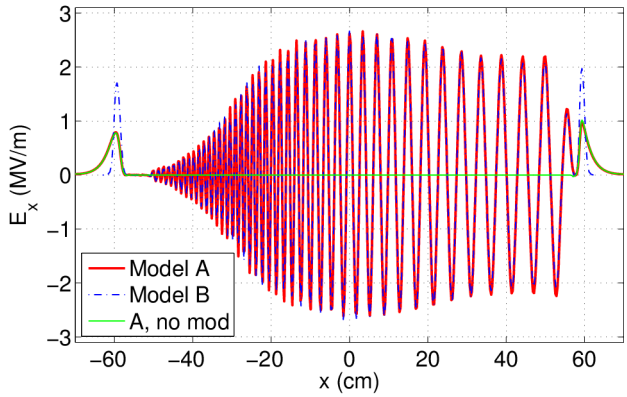

Figure 4: Longitudinal electric field in models A and B.

One important requirement for the RFQ operation is the inter-vane voltage flatness along the structure. Simulation results for model C are presented in Fig. 5 that shows relative voltages calculated at the midpoints of all 11 full periods. MWS results, both from eigensolvers with different meshes and in the time domain, coincide well but differ from measurements [2]. After additional MWS tuning [4], the MWS results are closer to measurements.

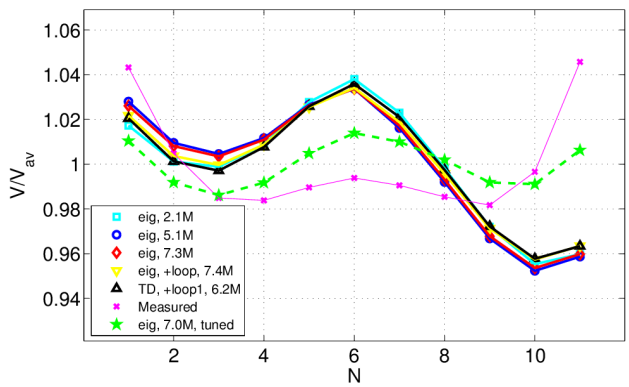

Figure 5: Voltage profile along the structure in model C.

The calculated maximal field at nominal voltage E_{max} = 31 MV/m ($2.1E_K$) is reached near the sharp vane ends. The total dissipated power in model C for ideal copper surfaces is 80 kW at 100% duty and is distributed as follows: 50% on stems, 28% on vanes, 21% on tuners, and less than 1% on the RFQ-vessel inner surface [4].

BEAM DYNAMICS RESULTS

One can estimate effects of the end-gap fields on the beam energy. The H^- beam is injected at 35 keV, i.e. with β_{in} = 0.0086, and accelerated to 750 keV, corresponding to β_{out} = 0.04. For the RF frequency 201.25 MHz, the wavelength λ = 148.97 cm. One can see in Fig. 4 that in model B the length of the end-gap peaks is ~3 cm, close to $\beta_{out}\lambda/2$ but a few times $\beta_{in}\lambda/2$. For model A, the end-gap

ISBN 978-3-95450-122-9

peaks are wider at least by a factor of two. The transit factors T for the entrance gaps are small, but for the exit gap in model B the maximal value of T is 0.81, thus the energy change can be up to 25 keV, see [4, 5] for details.

The RF fields calculated by MWS are imported into the Particle Studio (PS) PIC solver. For macro-particle simulations, we used matched distributions generated by PARMILA [8]. A matched 60-mA CW H^- beam of 10K macro-particles, one RF period long, was generated at the model boundary from Twiss-parameters that were back-traced from the match point at the RFQ vane entrance. The distribution is converted to CST PS format and injected for up to 70 RF periods. As an illustration, Fig. 6 shows macro-particles in model C with $V = 1.25V_0$ at t = 300 ns after the injection start. The total number of macro-particles at this moment is about 543K. The particle energy is indicated by color shown on the energy scale.

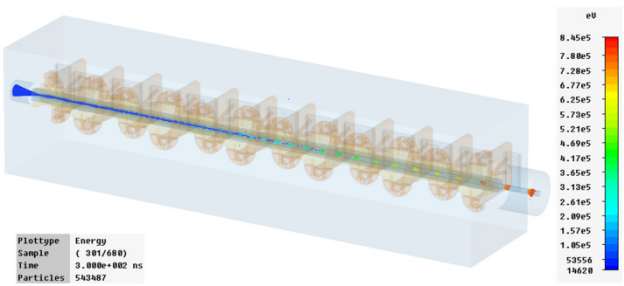

Figure 6: Macro-particles at t = 300 ns in the RFQ model C with increased inter-vane voltage, $V = 1.25V_0$.

A convenient way to look at energy changes is with phase-space snapshots of the longitudinal phase space x-W (coordinate-energy). In Fig. 4, five snapshots for model B, from t = 301 ns with 1-ns step, are overlapped. Each one is shown in a different color, and together they cover one RF period. The bunch energy increases until the end of the modulations (x = 570 mm), then drops in the end gap (588.7 to 600 mm), and remains constant in the exit beam pipe (x > 600 mm). On the contrary, there is no noticeable energy drop in model A [5].

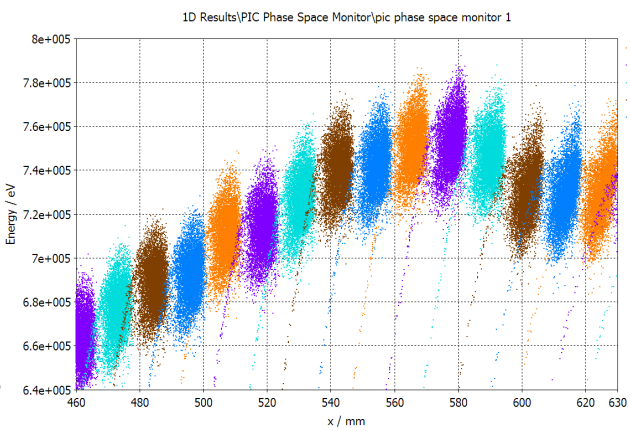

Figure 7: Phase-space near the RFQ exit in model B.

To exclude the effects of space charge in the head and tail of bunch trains, we analyzed only 50 central bunches from PS simulations with 70x10K beams injected. Some results with nominal and increased inter-vane voltages are shown in Table 1.

Table 1: PS Results for Models A and B

	Average energy, keV		Transmission	
RFQ model	A	B	A	B
$V = V_0$	750	729	0.91	0.93
$V = 1.25V_0$	753	729	0.89	0.97

The initial output beam energy of the FNAL RFQ in early 2012 was measured at 710 keV [2]. After our PS simulations demonstrated the energy effect of the end-gap fields, our colleagues at FNAL removed the output end plate of their RFQ (effectively moving from model B to A) and re-measured the output energy, obtaining 756 keV, near the design value [2]. In December 2012 they noticed that the beam exits the RFQ at an angle from -1° to -2° vertically. Following that, we analyzed data from our previous PS runs and confirmed this effect in simulations [5]. Our simulation results also suggest that the RFQ beam transmission depends strongly on input beam matching [5].

SUMMARY

A detailed study of the recently commissioned FNAL 4-rod RFQ was performed with the CST Studio codes. Of particular interest are effects associated with 3-D field asymmetries and end-gap fields, which are not predicted by standard RFQ design codes. The experience acquired in these CST simulations better prepares us to evaluate the performance of the new LANSCE 4-rod RFQ.

The authors would like to thank C.-Y. Tan (FNAL), A. Schempp and J. Schmidt (IAP, Frankfurt) for useful information and stimulating discussions.

REFERENCES

[1] R.W. Garnett et al, “Progress towards an RFQ-based front end for LANSCE,” IPAC2011, San Sebastian, WEPS068, p. 2658 (2011); http://www.JACoW.org
[2] C.-Y. Tan et al, PAC11, New York, p. 1701 (2011); also “FNAL RFQ Injector Upgrade Project” (2013), http://beamdocs.fnal.gov/AD-public/DocDB/ShowDocument?docid=3646
[3] CST Studio Suite, CST, 2012, www.cst.com
[4] S.S. Kurennoy, “EM modeling of 4-rod RFQs,” LA-UR-12-26388, Los Alamos, 2012.
[5] S.S. Kurennoy, “Beam dynamics modeling in RFQ with CST Particle Studio,” LA-UR-13-21653, Los Alamos, 2013.
[6] B. Koubek et al, PAC11, New York, p. 1888 (2011).
[7] P.N. Ostroumov et al., Phys. Rev. ST-AB, 15 (2012) 110101.
[8] Los Alamos Accelerator Code Group, laacg.lanl.gov.